J|A|C|S
ARTICLES
Published on Web 09/22/2006

Neutral and Zwitterionic Low-Coordinate Titanium Complexes Bearing the Terminal Phosphinidene Functionality. Structural, Spectroscopic, Theoretical, and Catalytic Studies Addressing the Ti−P Multiple Bond

Guangyu Zhao,[†] Falguni Basuli,[†] Uriah J. Kilgore,[†] Hongjun Fan,[†] Halikhedkar Aneetha,[†] John C. Huffman,[†] Gang Wu,[‡] and Daniel J. Mindiola*,[†]

Contribution from the Department of Chemistry and Molecular Structure Center, Indiana University, Bloomington, Indiana 47405, and Department of Chemistry, Queen's University, 90 Bader Lane, Kingston, Ontario, K7L3N6 Canada

Received July 7, 2006; E-mail: mindiola@indiana.edu

Abstract: α-Hydrogen abstraction and α-hydrogen migration reactions yield novel titanium(IV) complexes bearing terminal phosphinidene ligands. Via an α-H migration reaction, the phosphinidene ($^{t\text{Bu}}$nacnac)Ti═P[Trip]($CH_2{}^t$Bu) ($^{t\text{Bu}}$nacnac$^-$ = [Ar]NC(^{t}Bu)CHC(^{t}Bu)N[Ar], Ar = 2,6-$(CHMe_2)_2C_6H_3$, Trip = 2,4,6-$^i Pr_3C_6H_2$) was prepared by the addition of the primary phosphide LiPH[Trip] to the nucleophilic alkylidene triflato complex ($^{t\text{Bu}}$nacnac)Ti═CH^{t}Bu(OTf), while α-H abstraction was promoted by the addition of LiPH[Trip] to the dimethyl triflato precursor ($^{t\text{Bu}}$nacnac)Ti$(CH_3)_2$(OTf) to afford ($^{t\text{Bu}}$nacnac)Ti═P[Trip](CH_3). Treatment of ($^{t\text{Bu}}$nacnac)Ti═P[Trip](CH_3) with $B(C_6F_5)_3$ induces methide abstraction concurrent with formation of the first titanium(IV) phosphinidene zwitterion complex ($^{t\text{Bu}}$nacnac)Ti═P[Trip]$\{CH_3B(C_6F_5)_3\}$. Complex ($^{t\text{Bu}}$nacnac)-Ti═P[Trip]$\{CH_3B(C_6F_5)_3\}$ [2 + 2] cycloadds readily PhCCPh to afford the phosphametallacyclobutene [($^{t\text{Bu}}$nacnac)Ti(P[Trip]PhCCPh)][$CH_3B(C_6F_5)_3$]. These titanium(IV) phosphinidene complexes possess the shortest Ti═P bonds reported, have linear phosphinidene groups, and reveal significantly upfielded solution ^{31}P NMR spectroscopic resonances for the phosphinidene phosphorus. Solid state ^{31}P NMR spectroscopic data also corroborate with all three complexes possessing considerably shielded chemical shifts for the linear and terminal phosphinidene functionality. In addition, high-level DFT studies on the phosphinidenes suggest the terminal phosphinidene linkage to be stabilized via a pseudo Ti≡P bond. Linearity about the Ti−P−C_{ipso} linkage is highly dependent on the sterically encumbering substituents protecting the phosphinidene. Complex ($^{t\text{Bu}}$nacnac)Ti═P[Trip]$\{CH_3B(C_6F_5)_3\}$ can catalyze the hydrophosphination of PhCCPh with H_2PPh to produce the secondary vinylphosphine HP[Ph]PhC═CHPh. In addition, we demonstrate that this zwitterion is a powerful phospha-Staudinger reagent and can therefore act as a carboamination precatalyst of diphenylacetylene with aldimines.

Introduction

In contrast to imides, high-oxidation state transition metal phosphinidenes are still scant,[1−13] and such systems draw popularity given their ability to carry out important transformations such as phospha-Staudinger or -Wittig type reactions.[1−6] Specifically, phosphinidenes are particularly attractive synthons in the design of low-coordinate phosphorus in phosphaorganic molecules.[1−6] In the context of d^0-transition metal phosphinidenes,[4−9] the phosphinidene functionality is expected to be nucleophilic, and is often comparable in reactivity to Schrock-type alkylidenes since phosphorus is slightly more electropositive than carbon.[3]

[†] Indiana University.
[‡] Queen's University.

(1) Lammertsma, K.; Vlaar, M. J. M. *Eur. J. Org. Chem.* **2002**, 1127−1138.
(2) (a) Cowley, A. H. *Acc. Chem. Res.* **1997**, *30*, 445−451. (b) Cowley, A. H.; Barron, A. R. *Acc. Chem. Res.* **1988**, *21*, 81−87.
(3) Mathey, F. *Angew. Chem., Int. Ed.* **2003**, *42*, 1578−1604 and references therein.
(4) (a) Hou, Z. M.; Stephan, D. W. *J. Am. Chem. Soc.* **1992**, *114*, 10088−10089. (b) Hou, Z. M.; Breen, T. L.; Stephan, D. W. *Organometallics* **1993**, *12*, 3158−3167. (c) Breen, T. L.; Stephan, D. W. *J. Am. Chem. Soc.* **1995**, *117*, 11914−11921. (e) Stephan, D. W. *Angew. Chem., Int. Ed. Eng.* **2000**, *39*, 314−329. (f) Pikies, J.; Baum, E.; Matern, E.; Chojnacki, J.; Grubba, R.; Robaszkiewicz, A. *Chem. Commun.* **2004**, 2478−2478.
(5) Cummins, C. C.; Schrock, R. R.; Davis, W. M. *Angew. Chem., Int. Ed.* **1993**, *32*, 756−759.
(6) (a) Basuli, F.; Tomaszewski, J.; Huffman, J. C.; Mindiola, D. J. *J. Am. Chem. Soc.* **2003**, *34*, 10170−10171. (b) Basuli, F.; Watson, L. A.; Huffman, J. C.; Mindiola, D. J. *J. Chem. Soc., Dalton Trans.* **2003**, 4228−4229. (c) Bailey, B. C.; Huffman, J. C.; Mindiola, D. J.; Weng, W.; Ozerov, O. V. *Organometallics* **2005**, *24*, 1390−1393. (d) Basuli, F.; Bailey, B. C.; Huffman, J. C.; Baik, Mu-H.; Mindiola, D. J. *J. Am. Chem. Soc.* **2004**, *126*, 1924−1925.
(7) Urnezius, E.; Lam, K.-C.; Rheingold, A. L.; Protasiewicz, J. D. *J. Organomet. Chem.* **2001**, *630*, 193−197.
(8) Other Zr phosphinidene complexes have been isolated by trapping experiments. Mahieu, A.; Igau, A.; Majoral, J.-P. *Phosphorus Sulfur* **1995**, *104*, 235−239.
(9) Bonanno, J. B.; Wolczanski, P. T.; Lobkovsky, E. B. *J. Am. Chem. Soc.* **1994**, *116*, 11159−11160.
(10) A high oxidation state uranium phosphinidene has also been prepared. Arney, D. S. J.; Schnabel, R. C.; Scott, B. C.; Burns, C. J. *J. Am. Chem. Soc.* **1996**, *118*, 6780−6781.
(11) Hitchcock, P. B.; Lappert, M. F.; Leung, W. P. *J. Chem. Soc., Chem. Commun.* **1987**, 1282.
(12) Cowley, A. H.; Pellerin, B.; Atwood, J. L.; Bott, S. G. *J. Am. Chem. Soc.* **1990**, *112*, 6734−6735.
(13) Figueroa, J. S.; Cummins, C. C. *Angew. Chem., Int. Ed.* **2004**, *43*, 984−988.

Although phosphinidenes have been pursued as synthons for stoichiometric "PR" group transfer processes,[1−5] examples of phosphinidenes playing a role in catalytic reactions are exceedingly rare.[14] This fact is rather surprising since the closely related imides[15] and alkylidenes[16] are commonly sought catalysts in organotransition metal chemistry.

Unlike the 4d, 5d, and the late-transition metal series, titanium phosphinidenes were, until very recently, an unknown class of compounds.[6] One could attribute the lack of stable titanium phosphinidenes to be the result of the hard−soft contrast among these elements.[7,8] Theoretical studies by Lammertsma and coworkers have proposed that the nature of the nucleophilic M═P bond depends inter alia on the atomic size of the metal and not on the nature of the ligand.[17] Consequently, there is a much stronger σ- and π-component in the M═P interaction when moving from the first- to the second- and third-row transition metals.[17] Arguably, this would imply that Ti═P linkages are more reactive than its heavier group congeners.

In light of the above proposition, we wish to report the synthesis of the neutral and zwitterionic titanium(IV) phosphinidene complexes ($^{t\text{Bu}}$nacnac)Ti═P[Trip]($CH_2{}^t$Bu), ($^{t\text{Bu}}$nacnac)Ti═P[Trip](CH_3), ($^{t\text{Bu}}$nacnac)Ti═P[Trip]{$CH_3B(C_6F_5)_3$} ($^{t\text{Bu}}$nacnac$^-$ = [Ar]NC(^{t}Bu)CHC(^{t}Bu)N[Ar], Ar = 2,6-^{i}Pr$_2$C$_6$H$_3$, Trip = 2,4,6-^{i}Pr$_3$C$_6$H$_2$), as well as catalytic studies surrounding the Ti═P bond for the latent low-coordinate zwitterion ($^{t\text{Bu}}$nacnac)Ti═P[Trip]{$CH_3B(C_6F_5)$}. Solid-state structural studies reveal all these titanium phosphinidenes to possess the shortest Ti═P bonds ever reported, while ^{31}P NMR spectroscopic data (both in solution and solid state forms) indicate highly shielded ^{31}P NMR resonances for the terminal phosphinidene phosphorus. In addition, high-level DFT studies for all three titanium-phosphinidenes clearly depict the HOMO and HOMO-1 orbitals to be the two orthogonal π-bonds comprising the Ti≡P linkage. Bond order analysis corroborate the short Ti−P linkage with a bond order greater than two for all phosphinidene complexes studied in this work.

Results and Discussion

Synthesis and Structural Elucidation of Terminal Titanium Phosphinidene Complexes. Recently, we reported that four-coordinate titanium phosphinidenes could be generated via an α-hydrogen migration reaction involving the nucleophilic titanium alkylidene ($^{\text{Me}}$nacnac)Ti═CH^{t}Bu(OTf) ($^{\text{Me}}$nacnac$^-$ = [Ar]NC(Me)CHC(Me)N[Ar], Ar = 2,6-^{i}Pr$_2$C$_6$H$_3$) and the corresponding phosphide LiPH[R] (R = ^{c}C$_6$H$_{11}$, 2,4,6-^{i}Pr$_3$C$_6$H$_2$, 2,4,6-^{t}Bu$_3$C$_6$H$_2$).[6a] Unfortunately, these titanium phosphinidenes ($^{\text{Me}}$nacnac)Ti═P[R]($CH_2{}^t$Bu) were all kinetic products under N_2 inasmuch as these species readily underwent intramolecular phospha-Staudinger reactions (for R = ^{c}C$_6$H$_{11}$, 2,4,6-^{i}Pr$_3$C$_6$H$_2$) (Scheme 1).[6a] However, when R = 2,4,6-^{t}Bu$_3$C$_6$H$_2$, the titanium phosphinidene was moderately stable to isolate under low-temperature conditions, but gradual decomposition at room-temperature precluded us from carrying out more thorough analysis surrounding the nature of the Ti═P linkage. To block thermal rearrangement via a phospha-Staudinger reaction,[6a] we resorted to the much more sterically demanding β-diketiminate ligand version, ($^{t\text{Bu}}$nacnac$^-$ = [Ar]NC(^{t}Bu)CHC(^{t}Bu)N[Ar], Ar = 2,6-^{i}Pr$_2$C$_6$H$_3$), previously reported by Budzelaar and coworkers.[18] Accordingly, treatment of LiPH[Trip] with ($^{t\text{Bu}}$nacnac)Ti═CH^{t}Bu(OTf)[19] resulted in immediate formation of the phosphinidene ($^{t\text{Bu}}$nacnac)Ti═P[Trip]($CH_2{}^t$Bu) (Trip = 2,4,6-^{i}Pr$_3$C$_6$H$_2$ (**1**), 62% yield). Complex **1** is likely generated by means of a putative neopentylidene-phosphide ($^{t\text{Bu}}$nacnac)Ti═CH^{t}Bu(PH[Trip]), which subsequently undergoes α-hydrogen migration to afford the phosphinidene scaffold in **1** (Scheme 1). Attempts to transmetalate ($^{t\text{Bu}}$nacnac)Ti═CH^{t}Bu(OTf) with the aliphatic substituted phosphide LiPH[^{c}C$_6$H$_{11}$] or bulkier arylphosphide LiPH[2,4,6-^{t}Bu$_3$C$_6$H$_2$] resulted in decomposition mixtures. Given the steric protection imposed by the NCCCN β-carbon, complex **1** appears to be impervious to intramolecular phospha-Staudinger rearrangements often encountered with the more conventional $^{\text{Me}}$nacnac$^-$ system.[6a] The ^{1}H NMR spectrum of **1** displays two methine resonances, four diasteriotopic methyl groups on the isopropyls, as well as one ^{t}Bu environment for the β-carbons of the β-diketiminate backbone. As a result, all NMR spectroscopic data are consistent with complex **1** retaining C_s symmetry in solution. Most notably, the ^{31}P and ^{31}P{^{1}H} NMR solution spectra of **1** manifests a single resonance at 157 ppm, which is consistent with this system bearing a terminal and linear Ti═PR functionality. To our knowledge, complex **1** represents a rare example of a group 4 complex having a highly shielded ^{31}P NMR chemical shift for the phosphinidene phosphorus.[1−3] The highly shielded ^{31}P NMR resonance for **1** provided the impetus for examining the solid-state structure.

Scheme 1. Synthesis of the Titanium(IV) Phosphinidene **1** via an α-H Migration Reaction

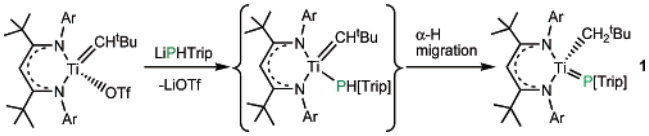

Large brown blocks of **1** were grown from hexane at −35 °C, and the single-crystal structure revealed a titanium complex having C_s symmetry, a Ti(IV)−C_{alkyl} bond (2.107(3) Å; Figure 1), and a short Ti═P bond (2.157(2) Å; Figure 1). As a result, the former metrical parameters reflect an α-hydrogen migration from the former primary phosphide ligand to the alkylidene carbon (Table 1). The Ti═P bond length value is by far much shorter to the computed Pauling and Schomaker−Stevenson covalent radii with corrections for electronegativity differences, which predicts a bond length of 2.288 Å for a double bond.[20] In the structure of **1**, the phosphinidene group is along the σ-plane bisecting N−Ti−N, and oriented syn with respect to the neopentyl ligand. A close interaction is also observed between the titanium center and the β-carbon forming part of the NCCCN ring (Ti1−C3, 2.638(4) Å). The metal center in **1** assumes its rightful position out of the NCCCN imaginary plane, therefore making the neopentyl group endo relative to the

(14) A phosphinidene anion has been implicated in the catalytic oligomerization of primary phosphines via dyhydrocoupling of P−H bonds. Fermin, M. C.; Stephan, D. W. *J. Am. Chem. Soc.* **1995**, *117*, 12645−12646.
(15) For some recent reviews of early-transition metal imides and their role in catalytic reactions. (a) Duncan, A. P.; Bergman, R. G. *Chem. Rec.* **2002**, *2*, 431−445. (b) Hazari, N.; Mountford, P. *Acc. Chem. Res.* **2005**, *38*, 839−849.
(16) (a) Schrock, R. R. *Chem. Rev.* **2002**, *102*, 145−179. (b) Schrock, R. R. *Acc. Chem. Res.* **1990**, *23*, 158−165.
(17) Ehlers, A. W.; Baerends, E. J.; Lammertsma, K. *J. Am. Chem. Soc.* **2002**, *124*, 2831−2838.
(18) Budzelaar, P. H. M.; von Oort, A. B.; Orpen, A. G. *Eur. J. Inorg. Chem.* **1998**, 1485−1494.
(19) Basuli, F.; Bailey, B. C.; Huffman, J. C.; Mindiola, D. J. *Organometallics* **2005**, *24*, 1886−1906.
(20) Pauling, L. *The Nature of the Chemical Bond*, 3rd ed.; Cornell University Press: Ithaca, NY, 1960.

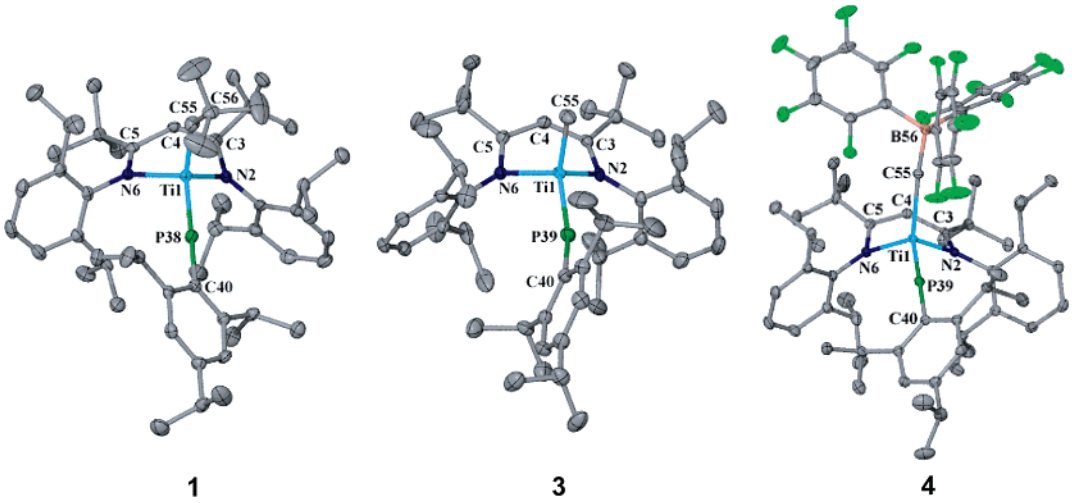

Figure 1. Crystal structures of complexes **1**, **3**, and **4** with thermal ellipsoids at the 50% probability level. H-atoms and solvent molecules have been removed for simplicity.

Table 1. Selected Structural Parameters for Complexes **1**, **3**, and **4**

complex	1	3	4
Ti═P	Ti(1)−P(39), 2.157(2)	Ti(1)−P(39), 2.1644(7)	Ti(1)−P(39), 2.1512(4)
Ti−N	Ti1−N2, 1.981(3)	Ti1−N2, 2.036(6)	Ti1−N2, 2.042(1)
Ti−N	Ti1−N6, 2.114(3)	Ti1−N7, 2.014(6)	Ti1−N6, 1.973(1)
Ti−C_α	Ti(1)−C(55), 2.107(3)	Ti(1)−C(55), 2.155(2)	Ti(1)−C(55), 2.405(3)
Ti−C_β	Ti(1)−C(3), 2.638(4)	Ti(1)−C(3), 2.720(2)	Ti(1)−C(3), 2.677(3)
Ti−C_β	n/a	Ti(1)−C(5), 2.665(2)	Ti(1)−C(5), 2.555(3)
Ti−C_γ	n/a	n/a	Ti(1)−C(4), 2.606(4)
C_α−B	n/a	n/a	C(55)−B(56), 1.665(2)
Ti−P−C	Ti(1)−P(39)-C(40), 176.64(7)	Ti(1)−P(39)-C(40), 159.95(7)	Ti(1)−P(39)-C(40), 176.03(5)
N−Ti−N	N(6)−Ti(1)-N(2), 98.8(1)	N(6)−Ti(1)-N(2), 98.78(6)	N(6)−Ti(1)-N(2), 99.33(4)
P−Ti−N	P39−Ti1−N2, 107.2(1)	P39−Ti1−N2, 107.57(5)	P39−Ti1−N2, 103.79(3)
P−Ti−N	P39−Ti1−N6, 109.29(9)	P39−Ti1−N6, 109.65(5)	P39−Ti1−N6, 108.11(3)
C_α−Ti−P	C(55)−Ti(1)-P(39), 112.2(1)	C(55)−Ti(1)-P(39), 111.26(8)	C(55)−Ti(1)-P(39), 112.57(4)
C_α−Ti−N	C(55)−Ti(1)-N(2), 116.05(9)	C(55)−Ti(1)-N(2), 115.68(8)	C(55)−Ti(1)-N(2), 113.19(5)
C_α−Ti−N	C(55)−Ti(1)-N(6), 112.38(9)	C(55)−Ti(1)-N(6), 113.14(9)	C(55)−Ti(1)-N(6), 118.20(5)
Ti−C_α−X	Ti1−C55−C56, 141.2(6)	n/a	Ti1−C55−B56, 175.44(10)

[a] Bond lengths are reported in Å and bond angles in deg. X represents the atoms carbon and boron for complexes **1** and **4**, respectively. n/a = not available.

isopropyl methyl groups. This feature places the linear phosphinidene group (Ti═P−C_{ipso}, 176.64(7)°) exo with respect to the isopropyl methyl residues. As expected, the linear phosphinidene ligand is in accord with the observed upfielded ^{31}P NMR chemical shift (vide supra).

Interestingly, it was discovered that titanium phosphinidenes could also be generated by an α-hydrogen abstraction reaction utilizing the precursor ($^{t\text{Bu}}$nacnac)Ti(CH_3)$_2$(OTf) (**2**) and LiPH[Trip]. Stephan[4a,c] and Protasiewicz[7] have applied this same strategy in the assembly of kinetically stable zirconium complexes bearing a terminal phosphinidene ligand. In a similar way, when an Et_2O solution of **2**, prepared readily from the AgOTf oxidation of ($^{t\text{Bu}}$nacnac)Ti(CH_3)$_2$ (Scheme 2),[21] was treated with LiPH[Trip], compound ($^{t\text{Bu}}$nacnac)Ti═P[Trip](CH_3) (Trip = 2,4,6-^{i}Pr$_3$C$_6$H$_2$; **3**) was isolated in 59% yield. Complex **3** also displays NMR spectroscopic features consistent with a C_s symmetric system in solution. A diagnostic terminal phosphinidene ^{31}P NMR chemical shift was located at 232 ppm, while the alkyl methyl group was unambiguously confirmed as a broad resonance at 1.27 ppm in the ^{1}H NMR spectrum. The alkyl methyl chemical shift in **3** coincides with the same group

Scheme 2. Synthesis of the Titanium Phosphinidene **3** via an α-H Abstraction Reaction of **2** with LiPH[Trip] and Subsequent Formation of the Zwitterion **4** by Methide Abstraction of **3** with $B(C_6F_5)_3$

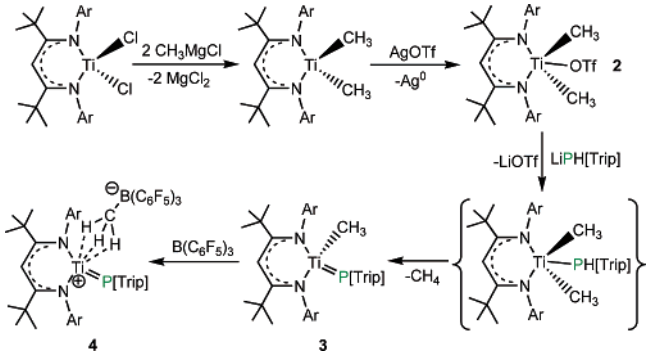

for the isoelectronic imido analogue ($^{t\text{Bu}}$nacnac)Ti═NR(CH_3) (R = 2,6-^{i}Pr$_2$C$_6$H$_3$), previously reported by our group (1.35 ppm).[22] We propose that complex **3** is likely formed by a transmetalation step to afford putative phosphide ($^{t\text{Bu}}$nacnac)-Ti(CH_3)$_2$(PH[Trip]) intermediate, which readily extrudes CH_4

(21) The analogous complex (^{Me}nacnac)Ti(CH_3)$_2$ has been reported by Budzelaar and co-workers, ref 15.

(22) (a) Basuli, F.; Clark, R. L.; Bailey, B. C.; Brown, D.; Huffman, J. C.; Mindiola, D. J. *Chem. Commun.* **2005**, 2250−2252. (b) Kilgore, U. J.; Basuli, F.; Huffman, J. C.; Mindiola, D. J. *Inorg. Chem.* **2006**, *45*, 487−489.

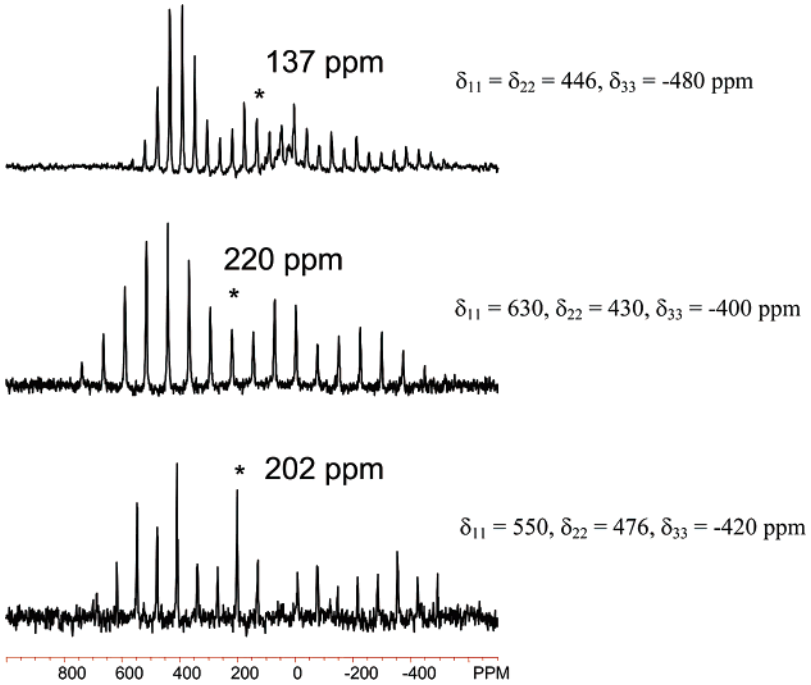

Figure 2. Solid-state ^{31}P MAS NMR spectra of complex **1** (top: 2084 transients, 8.737 kHz spinning), **3** (middle: 5050 transients, 15 kHz spinning), and **4** (bottom: 6140 transients, 14 kHz spinning). The isotropic peaks are indicated by asterisks. Tensors are reported to the right side of each spectrum.

upon α-hydrogen abstraction to furnish the Ti═P linkage (Scheme 2). Such a method allows us to assemble phosphinidene−methyl surrogates as opposed to the sterically encumbered phosphinidene−neopentyl groups in compounds such as (^{Me}nacnac)Ti═P[Trip]($CH_2{}^tBu$)[6a] (R = 2,4,6-^{t}Bu$_3$C$_6$H$_2$) or **1**.

To ascertain an accurate connectivity in compound **3**, we collected single-crystal X-ray diffraction data. Salient features for the structure of **3** include a very short Ti═P bond (2.1644(7) Å, Figure 1), and slightly distorted titanium phosphinidene group (Ti═P−C, 159.95(7)°), which is also oriented exo relative to the isopropyl methyl groups of the β-diketiminate ligand. Unlike the Ti═P−C motif in **1**, the phosphinidene group is not linear in **3**, hence hinting that sp hybridization of P in **1** might be sterically enforced and a consequence of clashing of the bulky aryl group on the phosphinidene P with both the neopentyl and sterically encumbering substitutents on the β-diketiminate ligand. As opposed to complex **1**, the less sterically imposing methyl group on Ti allows the phosphorus aryl motif to be oriented almost parallel to the imaginary NCCCN plane defined by the β-diketiminate ligand. Pertinent metrical parameters for the molecular structure of complex **3** are listed in Table 1.

Given the less-sterically congested environment in **3**, we decided to explore if such a complex could yield latent low-coordinate phosphinidene templates. As a result, treatment of **3** with B(C_6F_5)$_3$ in FC_6H_5 results in immediate methide abstraction concomitant with formation of the phosphinidene zwitterion (^{tBu}nacnac)Ti═P[Trip]{$CH_3B(C_6F_5)_3$} (**4**) in quantitative yield (Scheme 2). Diagnostic spectroscopic features for **4** include a ^{31}P NMR phosphinidene resonance at 207 ppm and a ^{11}B NMR spectroscopic signal at −14 ppm, both of which are consistent with a terminal phosphinidene zwitterion system resulting from methide abstraction. To our knowledge, complex **4** represents the first d^0 zwitterion featuring a terminal phosphinidene ligand. Although examples of cationic phosphinidene complexes have been reported by Carty,[23] high-oxidation state zwitterionic types were until now an unknown class of molecules.[4e,24]

In lieu of elemental analysis, and to obtain an accurate connectivity map for both the phosphinidene and zwitterionic nature of **4**, we collected single crystal X-ray diffraction data. Single-crystal X-ray diffraction analysis of **4** exposes a (^{tBu}nacnac)Ti═P[Trip] scaffold (Ti═P, 2.1512(4) Å; Ti═P−C, 176.03(5)°) with an abstracted methyl ligand (Ti−CH_3, 2.405(3) Å, Figure 1). Complex **4** contains a shorter Ti═P linkage and linear phosphinidene moiety when compared to **3**, thus hinting that a pseudo Ti≡P bond might be playing a role (Table 1). The perfluorinated aryls on the boron atom are twisted in a propeller like fashion and deviations of the boron atom from the aryl-C_3 plane (∼0.54 Å) lend further support to charge separation (or Lewis acid−base adduct formation) in **4**. As expected, methide abstraction in **4** results in an electron deficient and latent low-coordinate Ti(IV) center, consequently leading to a weak interaction of the latter with both the β- (2.677(3) and 2.555(3) Å) and γ-carbons (2.606(4) Å) composing the NCCCN ring (Table 1). The latter feature is further manifested by deviation of the Ti atom from the NCCCN imaginary plane (∼1.13 Å) when compared to **1** (∼1.01) and **3** (∼1.06). Complex **4** represents the pnictogen analogue of (^{tBu}nacnac)Ti═NR-{$CH_3B(C_6F_5)_3$} R = 2,6-^{i}Pr$_2$C$_6$H$_3$), a highly reactive zwitterionic titanium imido previously reported by us.[22]

Solid State ^{31}P NMR Spectroscopic Studies. Isotropic solid-state ^{31}P NMR shifts of the terminal phosphinidene complexes **1** (137 ppm), **3** (220 ppm), and **4** (202 ppm) obtained with

(23) (a) Sterenberg, B. T.; Carty, A. J. J. *Organomet. Chem.* **2001**, *617*−*618*, 696. (b) Sterenberg, B. T.; Udachin, K. A.; Carty, A. J. *Organometallics* **2001**, *20*, 2657−2659. (c) Sterenberg, B. T.; Udachin, K. A.; Carty, A. J. *Organometallics* **2001**, *20*, 4463−4465. (d) Sanchez-Nieves, J.; Sterenberg, B. T.; Udachin, K. A.; Carty, A. J. *J. Am. Chem. Soc.* **2003**, *125*, 2404−2405. (e) Sterenberg, B. T.; Udachin, K. A.; Carty, A. J. *Organometallics* **2003**, *22*, 3927−3932.
(24) Fermin, M. C.; Ho, J.; Stephan, D. W. *Organometallics* **1995**, *14*, 4247−4256.

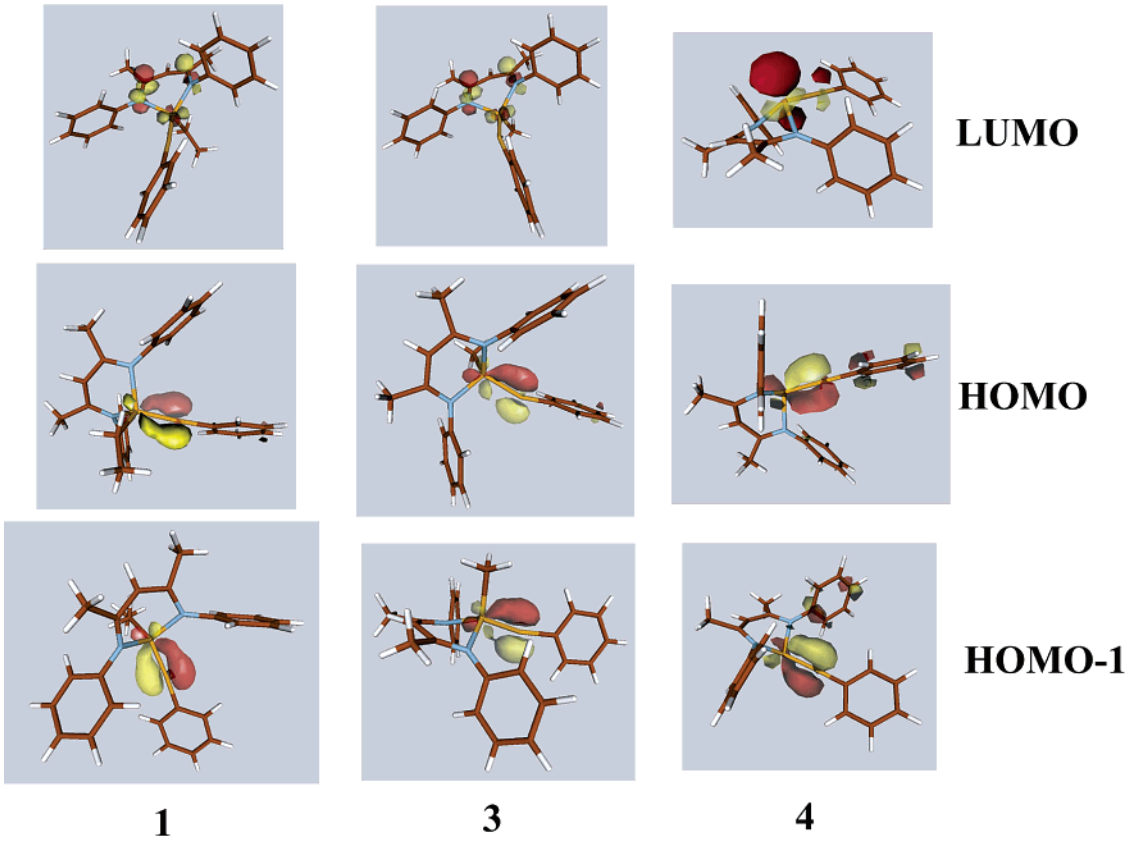

Figure 3. Computed frontier orbitals for the phosphinidene complexes **1**, **3**, and **4**. Full models have been cropped for drawing the orbitals: ^{t}Bu to CH_3 and ^{i}Pr to H.

Table 2. Selected Computed and X-ray Bond Distances (Å) and Bond Angles (deg) of the Full Models[a]

	compd 1		compd 3		compd 4	
atoms	calcd	X-ray	calcd	X-ray	calcd	X-ray
Ti1−P2	2.151	2.157	2.169	2.164	2.126	2.151
Ti1−C3	2.100	2.107	2.113	2.155	2.419	2.405
Ti1−N*	2.080	2.048	2.059	2.025	2.036	2.008
P2−C6	1.834	1.808	1.832	1.814	1.826	1.808
N4−Ti1−N5	97.7	98.82	98.0	98.8	99.0	99.33
Ti1−P2−C6	175.9	176.6	158.5	160.0	178.2	176.0

*Average of both Ti−N values.

magic-angle-spinning (MAS) are in agreement with the chemical shifts observed in solution (Figure 2). These isotropic resonances possess extended chemical shift anisotropies spread over a range of ∼900 ppm, and from the rotational sidebands the chemical shielding tensor components are obtained (Figure 2). On the basis of the chemical shielding anisotropies (CSA) observed for **1**, **3**, and **4**, it is clear that the small isotropic chemical shifts are primarily due to the fact that the tensor component along the Ti−P−C_{ipso} direction (δ_{33}) is significantly shielded. The latter value is relatively small when compared with the only phosphinidene case in the literature reporting ^{31}P CSA data, namely the trinuclear cluster *nido*-$Ru_4(CO)_{13}(\mu^3$-PPh) bearing a bridging phosphinidene ligand.[25] In fact, the solid-state isotropic ^{31}P chemical shifts found for the Ti=P compounds presented in this work are exceedingly shielded when compared to the solution ^{31}P NMR spectra of the few terminal terminal and linear phosphinidene complexes reported in the literature.[5,12] It is also well-known that linear and terminal phosphinidenes exhibit a much shielded environment than the corresponding bent analogues.[1−3,5,9,11,12] Hence, our solution and solid-state ^{31}P NMR data are consistent with linear Ti=P−C_{ipso} frameworks, which are also in agreement with the solid-state crystal structures (vide supra).

Computational Studies. To address the factors governing structure and bonding in complexes **1**, **3**, and **4**, we carried out theoretical calculations using high level density functional theory as implemented in the Jaguar 5.5 suite[26] of ab initio quantum chemistry programs. Geometry optimizations were performed with the B3LYP[27] functional and the 6-31G** basis set. Titanium was represented using the Los Alamos LACVP basis.[28] For all three phosphinidene complexes the optimized geometry for the full model reproduced the key features of the solid state structure expectedly well (Table 2). The structural features of **4** can also be reproduced accurately by simplifying the zwitterion to its cationic component ($^{t\text{Bu}}$nacnac)Ti=P[Trip], thus indicating that the $B(CH_3)(C_6F_5)_3$ anion has no significant structural influence to the core structure.

The frontier orbitals of complexes **1**, **3**, and **4** are shown in Figure 3. In all systems, the HOMO and HOMO-1 are composed

(25) (a) Eichele, K.; Wasylishen, R. E.; Corrigan, J. F.; Taylor, N. J.; Carty, A. J. *J. Am. Chem. Soc.* **1995**, *117*, 6961−6969. (b) Solid state ^{31}P NMR studies have been also reported for terminal tungsten and molybdenum phosphides. Wu, G.; Rovnyak, D.; Johnson, M. J. A.; Zanetti, N. C.; Musaev, D. G.; Morokuma, K.; Schrock, R. R.; Griffin, R. G.; Cummins, C. C. *J. Am. Chem. Soc.* **1996**, *118*, 10654−10655.

(26) *Jaguar*, 5.5 ed.; Schrödinger, L. L. C: Portland, OR, 1991−2003.

(27) (a) Becke, A. D. *Phys. Rev. A: At., Mol., Opt. Phys.* **1988**, *38*, 3098−3100. (b) Becke, A. D. *J. Chem. Phys.* **1993**, *98*, 5648−5652. (c) Lee, C. T.; Yang, W. T.; Parr, R. G. *Phys. Rev. B: Condens. Matter Mater. Phys.* **1988**, *37*, 785−789. (d) Vosko, S. H.; Wilk, L.; Nusair, M. *Can. J. Phys.* **1980**, *58*, 1200−1211.

(28) Mayer, I. *Chem. Phys. Lett.* **1983**, *97*, 270−274.

Table 3. Full Models versus Simplified Models: Calculated Bond Distances (Å), Bond Angles (deg), and the Mayer Bond Order

		compd 1		compd 3		compd 4	
	atoms	full	simplified	full	simplified	full	simplified
metrical parameter	Ti1−P2	2.151	2.24	2.169	2.26	2.126	2.24
	Ti1−P2−C6	175.9	106.4	158.5	95.9	178.2	68.5
bond order	Ti1−P2	2.11	1.87	2.06	1.76	2.26	1.81

of two orthogonal π-bonds invoking in the Ti−P linkage, and the calculated Mayer bond orders[29] for the Ti−P linkage are 2.06, 2.11, and 2.26 respectively (Table 3). These features clearly suggest that the linear Ti−P−C_{ipso} angle and short Ti−P distance result from a pseudo Ti≡P bond. The LUMO orbitals of complexes **1** and **3** are β-diketiminate π^* based augmented with some metal d character. However, drastic differences arise when the LUMO of **1** or **3** with that of the zwitterion **4** are compared. Not surprisingly, methide abstraction in **4** results in an open coordination site, hence the LUMO is composed primarily of a nonbonding metal-based orbital. This feature would suggest that complex **4** should be a system viable for substrate binding, since the LUMO orbital has large directionality along one lobe which is oriented toward the open coordination site.

Geometry optimizations of **1**, **3**, and **4** indicate that alterations of the all ^{i}Pr groups of the full models to H's or ^{t}Bu to CH_3 (the simplified model is displayed in Figure 3) result in considerable discrepancies in the Ti−P−C_{ipso} angles, together with elongation of Ti−P bond lengths (Table 3). Consequently, our computed bond orders (Table 3) for the simplified structures are more consistent with a Ti═P bond as opposed to the Ti≡P linkage suggested in Table 2. This perturbation implies that linearity at the Ti−P−C_{ipso} motif and the bonding scheme invoking the Ti−P linkage are possibly dominated by the sterically imposing substituents on the phosphinidene and β-diketiminate nitrogens. Clearly, a pseudo Ti≡P bond results in a lower energy species since the linear Ti−P−C_{ipso} linkage places both the P substituent outward to reduce the steric repulsion with the neopentyl group and sterically encumbering ^{t}Bu groups of the β-diketiminate ligand. Similar features involving the sterics at P have been discussed previously by our group.[6c] To form the Ti≡P bond, donation of the lone pair of P: → Ti needs to occur. Perplexed by the Ti═P bond order preference observed for the simplified models, we speculate that there must be a greater energy penalty for rearrangement to a linear Ti−P−C_{ipso} linkage than the energy gained from forming a pseudo-triple bond, Ti≡P.

Reactivity Studies of the Phosphinidene Zwitterion 4. Compounds **1** and **3** fail to react with diphenylacetylene presumably because of the sterically protected phosphinidene functionality. Complex **4** however, contains a labile borate group and would therefore be expected to be more reactive than its neutral derivatives. Hence, complex **4** reacts rapidly with PhCCPh to afford the phosphametallacyclobutene salt [($^{t\text{Bu}}$nacnac)Ti(P[Trip]PhCCPh)][$CH_3B(C_6F_5)_3$] (**5**) in >90% yields (Scheme 3). ^{31}P and ^{13}C NMR spectra are indicative of one isomer present, which contains a three-coordinate phosphorus species resulting from a [2 + 2] cycloaddition of the alkyne across the Ti═P bond (see Experimental Section). Stronger evidence for

Scheme 3. Cycloaddition of the Titanium(IV) Zwitterion Complex **4** with PhCCPh to Provide **5**, and Subsequent Protonation of the Metallacycle with H_2NPh to Afford the Secondary Vinylphosphine HP[Trip]PhC═CHPh

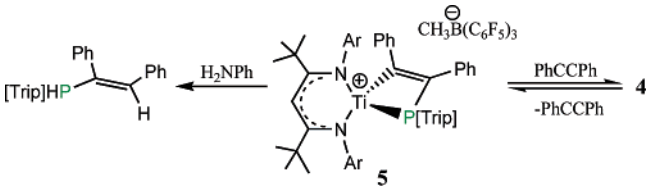

cycloadduct formation in **5** is provided by its reactivity with protic media such as H_2NPh, which results in extrusion of the secondary vinylphosphine HP[Trip]PhC═CHPh[30] (^{31}P NMR: −63.3 ppm, J_{P-H} = 221.9 Hz; MS (EI) M^+ = 414.25) concurrent with traces of the free phosphine H_2P[Trip] (Scheme 3). We have been unable to identify the metal-based product resulting from protonolysis, but separation of HP[Trip]PhC═CHPh from the mixture is facile given the limited solubility of the metal byproduct in hydrocarbons. When judging from the ^{31}P NMR spectrum, no isomer or phosphaalkene tautomer is present with the secondary vinylphosphine. However, the presence of some free phosphine suggests that complex **5** might be in equilibrium with **4** and PhCCPh. Similar equilibrium processes have been observed with azatitanocyclobutene species generated from PhCCPh and the corresponding metal-imide.[31,32] Albeit rare, stable phosphametallacyclobutene complexes of zirconium have been previously reported by Stephan and coworkers.[33] These systems also [2 + 2] retrocycloadd the alkyne, since tertiary phosphines cleanly transform the phosphametallacyclobutene to the corresponding phosphinidene phosphine adduct and the free alkyne.[33]

Catalytic Activity of Terminal Titanium Phosphinidenes. Given the ability of **4** to undergo [2 + 2] cycloaddition with PhCCPh to afford the phosphametallacyclobutene, we reasoned that complex **4** could be poised to be a catalytic "PAr" transfer reagent. Accordingly, when **4** (10 mol %) was treated with PhCCPh and H_2PPh in C_6D_6 at 80 °C for 12 h, the secondary vinylphosphine HP[Ph]PhC═CHPh was isolated in 73% yield

(29) (a) Hay, P. J.; Wadt, W. R. *J. Chem. Phys.* **1985**, *82*, 270−283. (b) Wadt, W. R.; Hay, P. J. *J. Chem. Phys.* **1985**, *82*, 284−298.

(30) This type of secondary vinylphosphine is unknown but the 1-phosphaallyl anion [Aryl]PC(Ph)C(H)Ph (aryl = 2,4,6-^{t}Bu$_3$C$_6$H$_2$) has been reported. Niecke, E.; Nieger, M.; Wenderoth, P. *J. Am. Chem. Soc.* **1993**, *115*, 6989−6990. Secondary vinylphosphines of the type H_2C═CHPHR have also been reported. Gaumont, A. C.; Morise, X.; Denis, J. M. *J. Org. Chem.* **1992**, *57*, 4292−4295.

(31) The imide zwitterion ($^{t\text{Bu}}$nacnac)Ti═NR{$CH_3B(C_6F_5)_3$} (R = 2, 6-^{i}Pr$_2$C$_6$H$_3$) and PhCCPh are in equilibrium with the azametallacyclobutene complex [($^{t\text{Bu}}$nacnac)Ti(NRPhCCPh)][$CH_3B(C_6F_5)_3$]. Basuli, F.; Aneetha, H.; Huffman, J. C.; Mindiola, D. J. *J. Am. Chem. Soc.* **2005**, *127*, 17992−17993.

(32) (a) Baranger, A. M.; Walsh, P. J.; Bergman, R. G. *J. Am. Chem. Soc.* **1993**, *115*, 2753−2763. (b) Walsh, P. J.; Baranger, A. M.; Bergman, R. G. *J. Am. Chem. Soc.* **1992**, *114*, 1708−1719.

(33) (a) Breen, T. L.; Stephan, D. W. *J. Am. Chem. Soc.* **1996**, *118*, 4204−4205. (b) Breen, T. L.; Stephan, D. W. *Organometallics* **1996**, *15*, 5729−5737. (c) Transient ruthenium phosphametallacyclobutenes originated from alkynes have been proposed as likely intermediates in the formation of phosphaallyl moieties. (d) Termaten, A. T.; Nijbacker, T.; Schakel, M.; Lutz, M.; Spek, A. T.; Lammertsma, K. *Chem.—Eur. J.* **2003**, *9*, 2200−2208.

Scheme 4. Catalytic Hydrophosphination Utilizing the Phosphinidene Precatalyst **4**[a]

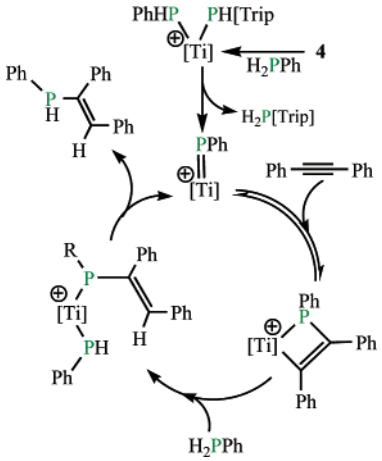

[a] The β-diketiminate ligand and $BCH_3(C_6F_5)_3$ anion are not shown for clarity. Formation of the cationic phenylphosphinidene catalyst [Ti]=PPh from **4** is proposed to occur via protonation and subsequent α-hydrogen abstraction steps.

as a pale yellow oil. Compound HP[Ph]PhC=CHPh forms as a monomer (MS (CI) $MH^+ = 289.11$) containing a mixture of *E* and *Z* isomers in a 5:2 ratio when judged by ^{31}P NMR spectroscopy and GC−MS. ^{31}P NMR (proton coupled) spectra of HP[Ph]PhC=CHPh clearly reveals not only coupling of the phosphorus to the proximal hydrogen ($^1J_{P-H} = 218-224$ Hz), but substantial coupling to the two ortho phenyl hydrogens ($^3J_{P-H} \sim 6$ Hz) as well as the vinylic hydrogen ($^3J_{P-H} = 14-17$ Hz). Compound HP[Ph]PhC=CHPh is a pale yellow oil which is exceedingly reactive toward air and slowly decomposes overtime to a mixture of products. A mechanism qualitatively similar to the more common, intermolecular catalytic hydroamination of alkynes appears likely to be operative for the system studied herein (Scheme 4). We propose that H_2PPh protonates the phosphinidene ligand in **4** to form a bisphosphide intermediate, which subsequently undergoes α-hydrogen abstraction to form the catalyst having a Ti=PPh linkage (Scheme 4). Evidence for phosphametallacyclobutene formation as opposed to the known 1,2-insertion mechanism[34] appears to be the favored route in this process since complex **4** fails to form a phosphine product when treated with $HPPh_2$ and PhCCPh under similar conditions.[35]

Given the ability of **4** to catalytically generate the secondary phosphine, we reasoned that this species was also suitable as a low-coordinate "($^{t\text{Bu}}$nacnac)Ti^{3+}" vehicle rather than a stoichiometric or catalytic phospha-Staudinger PAr delivery reagent. In other words, the propensity of **4** to undergo PAr group-transfer renders this complex a convenient precursor for other terminal functionalities confined in a low-coordination environment. Hence, one obvious functionality to conceive from the phosphinidene group is the imide, since early-transition metal complexes possessing this functionality play important roles in

Table 4. Carboamination Reactions to Prepare α,β-Unsaturated Imines[a]

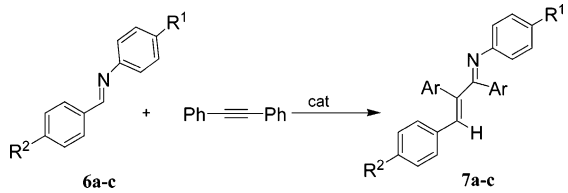

entry	aldimine	product	yield (%)
1	6a; $R^1 = CH_3$, $R^2 = CH_3$	7a	68
2[b]	6b; $R^1 = CH_3$, $R^2 = NMe_2$	7b	70
3	6c; $R^1 = OCH_3$, $R^2 = NMe_2$	7c	68

[a] Reactions were carried out with 10 mol % catalyst in C_6D_6 at 135 °C. Yield of the isolated product after column chromatography. [b] 5 mol % catalyst was used.

exciting intermolecular transformations such as the hydroamination of alkynes[32,36−43] and alkenes,[44] hydrohydrazination of alkynes,[45] three-component coupling reactions to form α,β-unsaturated β-iminoamines,[46] guanylation of amines,[47] and more recently carboamination,[31,48,49] among other catalytic processes.[15] Given our interest in catalytic carboamination,[31,49] a process in which an alkyne inserts into an aldimine C=N bond to form an α,β-unsaturated imine, we reasoned whether complex **4** could behave as an active precatalyst for this type of reaction.

Accordingly, when PhCCPh and corresponding aldimine where heated at 135 °C with 5−10 mol % of **4**, carboamination proceeded smoothly to afford the α,β-unsaturated imine in ∼70% isolated yield (Table 4). All highly arylated α,β-unsaturated imines had exclusive (*E*,*E*)-configuration at the olefin and imine residues according to Table 4. Generation of the α,β-unsaturated imine is proposed to occur initially by phospha-Staudinger metathesis of **4** with the aldimine to generate the putative phosphaalkene [Trip]P=CHR′ and the low-coordinate imide ($^{t\text{Bu}}$nacnac)Ti=NR{$CH_3B(C_6F_5)_3$}. While the former byproduct appears to be kinetically incompetent through-

(34) Catalyzed intramolecular hydrophosphination of alkenes and alkynes involving organolanthanide complexes have been reported. (a) Douglass, M. R.; Marks, T. J. *J. Am. Chem. Soc.* **2000**, *122*, 1824−1825. (b) Kawaoka, A. M.; Douglass, M. R.; Marks, T. J. *Organometallics* **2003**, *22*, 4630−4632. (c) Motta, A.; Fragala, I. L.; Marks, T. J. *Organometallics* **2005**, *24*, 4995−5003. (d) Douglass, M. R.; Stern, C. L.; Marks, T. J. *J. Am. Chem. Soc.* **2001**, *123*, 10221−10238.

(35) Intermolecular hydrophosphination of alkynes with $HPPh_2$ has been reported. Ohmiya, H.; Yorimitsu, H.; Oshima, K. *Angew. Chem., Int. Ed.* **2005**, *44*, 2368−2370 and references therein.

(36) (a) Anderson, L. L.; Arnold, J.; Bergman, R. G. *Org. Lett.* **2004**, *6*, 2519−2522. (b) Lee, S. Y.; Bergman, R. G. *Tetrahedron* **1995**, *51*, 4255−4276. (b) Ackermann, L. *Organometallics* **2003**, *22*, 4367−4368. (c) Straub, B. F.; Bergman, R. G. *Angew. Chem., Int. Ed.* **2001**, *40*, 4632−4635.

(37) Lorber, C.; Choukroun, R.; Vendier, L. *Organometallics* **2004**, *23*, 1845−1850.

(38) Ward, B. D.; Maisse-Francois, A.; Mountford, P.; Gade, L. H. *Chem. Commun.* **2004**, 704−705.

(39) Tillack, A.; Jiao, H.; Castro, I. G.; Hartung, C. G.; Beller, M. *Chem.−Eur. J.* **2004**, *10*, 2409−2420 and references therein.

(40) (3) Hill, J. E.; Profilet, R. D.; Fanwick, P. E.; Rothwell, I. P. *Angew. Chem., Int. Ed. Engl.* **1990**, *29*, 664−665.

(41) (a) Haak, E.; Bytschkov, I.; Doye, S. *Angew. Chem., Int. Ed.* **1999**, *38*, 3389−3391. (b) Pohlki, F.; Bytschkov, I.; Siebeneicher, H.; Heutling, A.; König, W. A.; Doye, S. *Eur. J. Org. Chem.* **2004**, 1967−1972. (c) Pohlki, F.; Doye, S. *Angew Chem., Int. Ed.* **2001**, *40*, 2305−2308. (d) For a review on hydroamination reactions involving alkynes: Pohlki, F.; Doye, S. *Chem. Soc. Rev.* **2003**, *32*, 104−114.

(42) Ong, T.-G.; Yap, G. P. A.; Richeson, D. S. *Organometallics* **2002**, *21*, 2839−2841.

(43) Zhang, Z.; Schafer, L. L. *Org. Lett.* **2003**, *5*, 4733−4736 and references therein.

(44) Ackermann, L.; Kaspar, L. T.; Gschrei, C. *J. Org. Lett.* **2004**, *6*, 2515−2518.

(45) (a) Odom, A. *J. Chem. Soc., Dalton Trans.* **2005**, 225−233 and references therein. (b) Li, Y.; Shi, Y.; Odom, A. L. *J. Am. Chem. Soc.* **2004**, *126*, 1794−1803.

(46) Cao, C.; Shi, Y.; Odom, A. L. *J. Am. Chem. Soc.* **2003**, *125*, 2880−2881.

(47) Ong, T.-G.; Yap, G. P. A.; Richeson, D. S. *J. Am. Chem. Soc.* **2003**, *125*, 8100−8101.

(48) (a) Ruck, R. T.; Zuckermann, R. L.; Krska, S. W.; Bergman, R. G. *Angew. Chem., Int. Ed.* **2004**, *43*, 5372−5374. (b) Ruck, R. T.; Bergman, R. G. *Organometallics* **2004**, *23*, 2231−2233.

(49) Aneetha, H.; Basuli, F.; Huffman, J. C.; Mindiola, D. J. *Organometallics* **2006**, *25*, 2402−2404.

Scheme 5. Catalytic Carboamination of Diphenylacetylene with Aryl Aldimines Utilizing the Phosphinidene Precatalyst **4**[a]

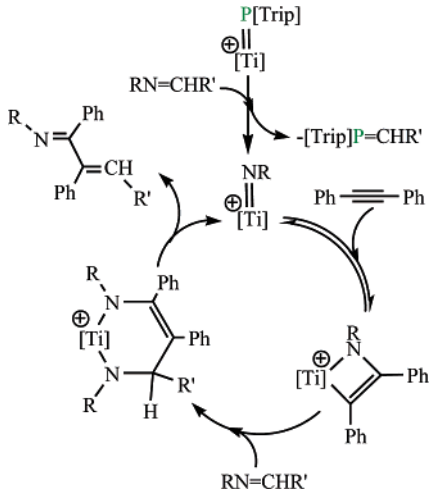

[a] The β-diketiminate ligand and $BCH_3(C_6F_5)_3$ anion are not shown for clarity.

out the catalytic process via dimerization or oligomerization, the latter subsequently undergoes [2 + 2] cycloaddition of the internal alkyne to provide the azametallacyclobutene [(*t*Bunacnac)-TiNRCPhCPh][$BCH_3(C_6F_5)_3$]. The azametallacyclobutene intermediate then inserts the aldimine to yield a thermally unstable six-membered ring metallacycle, which experiences [4 + 2] retrocycloaddition to regenerate the Ti═NR linkage and extrude the α,β-unsaturated imine (Scheme 5).

Conclusions

In summary, kinetically stable, neutral and zwitterionic phosphinidene complexes of titanium(IV) have been prepared. The Ti═P linkage can be generated by two independent routes, one via α-hydrogen migration, while the second synthetic approach applies α-hydrogen abstraction. The phosphinidene complexes reported in this paper contain exceedingly short Ti═P distances, linear Ti−P−C_{ipso} linkages, and highly shielded ^{31}P NMR resonances. These are the first terminal transition metal phosphinidenes to be elucidated by a combination of single-crystal X-ray diffraction, solid-state and solution ^{31}P NMR, and DFT analysis. On the basis of both solid-state structural and DFT studies, we propose that part of the stability of the titanium−phosphorus linkage arises from steric protection and not the formation of a pseudo Ti≡P bond since linearity at the Ti−P−C linkage in systems such as **1** could originate from clashing of the phosphorus sterically demanding aryl motif with other sterically demanding ligands such as neopentyl or bulky groups on the β-diketiminate ligand. Although Ti≡P formation is not prerequisite for these systems, spectroscopic, structural, and theoretical data point to a pseudo-triple bond between Ti and P which is operative for all the phosphinidenes systems presented in this work. We have demonstrated that a zwitterionic titanium complex possessing a terminal phosphinidene functionality can deliver the phosphinidene group in a catalytic fashion to generate the secondary vinylphosphine HP[Ph]PhC═CHPh. Taking advantage of the reactive nature of the Ti═P linkage we can also generate other functionalities capable of mediating other catalytic reactions such as the carboamination of diphenylacetylene with aldimines. Our work demonstrates for the first time that an early-transition M═P functionality can play a vital role in attractive catalytic processes such as the intermolecular hydrophosphination and carboamination of diphenylacetylene. We are currently exploring the intermolecular hydrophosphination of alkynes with primary phosphines catalyzed by titanium phosphinidenes, since secondary vinylphosphines have been demonstrated to tautomerize to the corresponding phosphaalkene.[50,51] The latter type of transformation would allow a facile entry to low-coordinate phosphaalkene moieties directly from the alkyne and the primary phosphine.

Experimental Section

General Considerations. Unless otherwise stated, all operations were performed in a M. Braun Lab Master double-drybox under an atmosphere of purified nitrogen or using high vacuum standard Schlenk techniques under an argon atmosphere.[52] Anhydrous n-hexane, pentane, toluene, and benzene were purchased from Aldrich in sure-sealed reservoirs (18 L) and dried by passage through two columns of activated alumina and a Q-5 column.[53] Diethyl ether was dried by passage through a column of activated alumina.[53] FC_6H_5 was purchased from Aldrich, degassed, and dried by passage though a column of activated alumina. THF was distilled, under nitrogen, from purple sodium benzophenone ketyl and stored under sodium metal. Distilled THF was transferred under vacuum into bombs before being pumped into a drybox. C_6D_6 was purchased from Cambridge Isotope Laboratory (CIL), degassed, dried over CaH_2, and vacuum transferred to 4 Å molecular sieves. THF-d_8 was purchased from CIL and stored over a sodium film. Celite, alumina, and 4 Å molecular sieves were activated under vacuum overnight at 200 °C. BrC_6D_5 was purchased from CIL and dried over activated alumina. $B(C_6F_5)_3$ was purchased from Boulder Scientific and sublimed under reduced pressure prior to use. Li(*t*Bunacnac) (*t*Bunacnac = [Ar]NC(*t*Bu)CHC(*t*Bu)N[Ar], Ar = 2,6-$(CHMe_2)_2C_6H_3$),[18] $LiCH_2{}^tBu$,[54] (*t*Bunacnac)$TiCl_2$,[19] (*t*Bunacnac)Ti═CH*t*Bu(OTf),[19] LiPH[Trip] (Trip = 2,4,6-$(CHMe_2)_3C_6H_2$),[55−57] were prepared according to the literature. All other chemicals were used as received. CHN analyses were performed by Desert Analytics, Tucson, AZ. ^{1}H, ^{13}C, ^{31}P, and ^{11}B NMR spectra were recorded on Varian 400 or 300 MHz NMR spectrometers. ^{1}H and ^{13}C NMR are reported with reference to solvent resonances (residual C_6D_5H in C_6D_6, 7.16 and 128.0 ppm; proteo THF in THF-d_8, 3.58, 1.73, and 67.4, 25.3; C_6H_5Br in C_6D_5Br 7.33, 7.05, 6.97 and 131.1, 129.6, 126.4, 122.4 ppm). ^{31}P NMR chemical shifts are reported with respect to external H_3PO_4 (aqueous solution, δ 0.0 ppm). ^{11}B NMR chemical shifts are reported with respect to external $BF_3{\cdot}OEt_2$ (δ 0.0 ppm). Solution magnetic moments were obtained by the method of Evans.[58] Electronic absorption spectra were obtained with a Perkin-Elmer Lamba 19 spectrophotometer using UVWinlab software. Single-crystal X-ray diffraction data were collected on a SMART6000 (Bruker) system under a stream of N_2(g) at low temperatures. Solid-state NMR spectra were obtained on a Bruker Avance-500 NMR spectrometer operating at 500.13 and 202.42 MHz for ^{1}H and ^{31}P nuclei, respectively. All ^{31}P chemical shifts were referenced to 85% H_3PO_4(aq) using a solid sample of $NH_4H_2PO_4$ as a secondary external reference. Powder samples

(50) Mercier, F.; Hugel-Le Goff, C.; Mathey, F. *Tetrahedron Lett.* **1989**, *30*, 2397−2398.
(51) Yam, M.; Tsang, C.-W.; Gates, D. P. *Inorg. Chem.* **2004**, *43*, 3719−3723.
(52) For a general description of the equipment and techniques used in carrying out this chemistry see: Burger, B. J.; Bercaw, J. E. In *Experimental Organometallic Chemistry*; Wayda, A. L., Darensbourg, M. Y., Eds.; ACS Symposium Series 357; American Chemical Society: Washington DC, 1987; pp 79−98.
(53) Pangborn, A. B.; Giardello, M. A.; Grubbs, R. H.; Rosen, R. K.; Timmers, F. J. *Organometallics* **1996**, *15*, 1518−1520.
(54) Schrock, R. R.; Fellmann, J. D. *J. Am. Chem. Soc.* **1978**, *100*, 3359−3370.
(55) Dias, H. V.; Power, P. P. *J. Am. Chem. Soc.* **1989**, *111*, 144−148.
(56) Kurz, S.; Hey-Hawkins, E. *Organometallics* **1992**, *11*, 2729−2732.
(57) (a) Cowley, A. H.; Kilduff, J. E.; Newman, T. H.; Pakulski, M. *J. Am. Chem. Soc.* **1982**, *104*, 5820−5821. (b) Cowley, A. H.; Norman, N. C.; Pakulski, M. *Inorg. Synth.* **1990**, *27*, 235−240.
(58) (a) Sur, S. K. *J. Magn. Reson.* **1989**, *82*, 169−173. (b) Evans, D. F. *J. Chem. Soc.* **1959**, 2003−2005.

were packed into zirconium oxide rotors (4 mm o.d.) in a drybox. Typical sample spinning frequencies for the MAS experiments are 8−15 kHz. The recycle time was 10 s and all spectra were recorded with cross polarization (2 ms contact time) and TPPM proton decoupling (70 kHz B_1 field). Variable sample spinning frequencies were used to identify the isotropic peak in each spectrum.

Synthesis of Complex ($^{t\mathrm{Bu}}$nacnac)Ti═P[Trip](CH$_2$^{t}Bu) (1). In a vial was dissolved ($^{t\mathrm{Bu}}$nacnac)Ti═CH^{t}Bu(OTf) [100 mg, 0.13 mmol] in Et_2O (10 mL), and the solution was cooled to −35 °C. To the cold solution was added an ether solution (∼5 mL) containing LiPH[Trip] [32 mg, 0.13 mmol]. After stirring for 30 min the solution was dried under reduced pressure. The brown powder was extracted with hexane and filtered, and the filtrate was concentrated and cooled to −35 °C to afford in two crops purple crystals of ($^{t\mathrm{Bu}}$nacnac)Ti═P[Trip](CH$_2$^{t}Bu) (**1**) [72 mg, 0.08 mmol, 61.5% yield].^{1}H NMR (23 °C, 399.8 MHz, C_6D_6): δ 7.05−6.74 (m, C_6H_3, C_6H_2, 8H), 5.39 (s, C(^{t}Bu)C*H*C(^{t}Bu), 1H), 4.14 (septet, C*H*Me$_2$, 2H), 3.59 (septet, C*H*Me$_2$, 2H), 3.30 (septet, C*H*Me$_2$, 2H), 2.60 (septet, C*H*Me$_2$, 1H), 1.68 (d, CH*Me*$_2$, 6H), 1.58 (s, Ti−CH$_2$^{t}*Bu*, 9H), 1.56 (s, Ti-*CH*$_2$^{t}Bu, 2H), 1.39 (d, CH*Me*$_2$, 6H), 1.28 (d, CH*Me*$_2$, 6H), 1.24 (d, CH*Me*$_2$, 6H), 1.08 (d, CH*Me*$_2$, 6H), 1.05 (s, C(*^{t}Bu*)CHC(*^{t}Bu*),18H), 1.01 (d, CH*Me*$_2$, 12H). ^{13}C NMR (25 °C, 100.6 MHz, C_6D_6): δ.173.0 (*C*(^{t}Bu)CH*C*(^{t}Bu)), 154.5 (ipso-C_6H_2, J_{C-P} = 28 Hz), 150.3 (C_6H_3), 149.5 (C_6H_3), 146.3 (C_6H_3), 141.8 (C_6H_3), 140.0 (C_6H_3), 137.1 (C_6H_3), 126.1 (C_6H_3), 124.6 (C_6H_3), 123.7 (C_6H_3), 98.3 (Ti-*C*H$_2$^{t}Bu, J_{C-H} = 100 Hz), 87.8 (C(^{t}Bu)*C*HC(^{t}Bu)), J_{C-H} = 151), 45.1 (C(*C*Me$_3$)CHC(*C*Me$_3$)), 36.9 (Ti−CH$_2$*C*Me$_3$), 35.5 (Ti−CH$_2$C*Me*$_3$), 34.4 (*C*HMe$_2$), 32.2 (*C*HMe$_2$), 31.8 (C(C*Me*$_3$)CHC(C*Me*$_3$)), 29.2 (*C*HMe$_2$), 28.7 (*C*HMe$_2$), 28.2 (*Me*), 27.7 (*Me*), 26.0 (*Me*), 24.9 (*Me*), 24.7 (*Me*), 24.5 (*Me*), 24.0 (*Me*). ^{31}P NMR (25 °C, 161.9 MHz, C_6D_6): δ 157.0 (s, *P*[Trip]). Anal. Calcd for $C_{55}H_{87}N_2TiP$: C, 77.25; H, 10.25; N, 3.28. Found: C, 76.93; H, 10.56; N, 3.20. UV−vis (C_7H_8, 25 °C): 319 (ϵ = 25344 L·mol^{-1}·cm^{-1}), 365 (ϵ = 13915 L·mol^{-1}·cm^{-1}), 490 (br shoulder) nm.

Synthesis of ($^{t\mathrm{Bu}}$nacnac)Ti(CH$_3$)$_2$. In a reaction vessel was dissolved ($^{t\mathrm{Bu}}$nacnac)$TiCl_2$ [2.04 g, 3.29 mmol] in hexane (50 mL) and the solution cooled to −35 °C. To the cold solution was added an ether solution containing CH_3MgCl [2.19 mL, 6.57 mmol]. After stirring for 20 min the solution was filtered, and the filtrate was concentrated under reduced pressure, and cooled to −35 °C to afford in two crops green crystals of ($^{t\mathrm{Bu}}$nacnac)Ti(CH$_3$)$_2$ (**2**) [1.339 g, 2.31 mmol, 70.3% yield]. ^{1}H NMR (23 °C, 399.8 MHz, C_6D_6): δ 6.12 ($\Delta\nu_{1/2}$ = 363 Hz), 5.50 ($\Delta\nu_{1/2}$ = 330 Hz), 4.90 ($\Delta\nu_{1/2}$ = 72 Hz), 2.46 ($\Delta\nu_{1/2}$ = 69 Hz); μ_{eff} = 1.85 μ_B (C_6D_6, 298 K, Evans' method). Anal. Calcd for $C_{37}H_{59}N_2Ti$: C, 76.65; H, 10.26; N, 4.83. Found: C, 76.94; H, 10.61; N, 4.80.

Synthesis of ($^{t\mathrm{Bu}}$nacnac)Ti(CH$_3$)$_2$(OTf) (2). In a vial was dissolved ($^{t\mathrm{Bu}}$nacnac)Ti(CH$_3$)$_2$ [1.00 g, 1.73 mmol] in THF (10 mL) and the solution was cooled to −35 °C. To the cold solution was added a THF solution (∼10 mL) containing AgOTf [443 mg, 1.73 mmol] causing precipitation of Ag^0. After stirring for 15 min the solution was filtered, the filtrate was dried under reduced pressure and was washed several times with hexane to afford ($^{t\mathrm{Bu}}$nacnac)Ti(CH$_3$)$_2$(OTf) (**3**) [952 mg, 1.31 mmol, 75.7% yield] as an orange solid. ^{1}H NMR (23 °C, 399.8 MHz, THF-d_8): δ 7.11−7.21 (m, C_6H_3, 6H), 6.47 (s, C(^{t}Bu)C*H*C(^{t}Bu), 1H), 3.34−3.60 (br, C*H*Me$_2$, 4H), 1.77 (s, *Me*$_2$Ti, 3H), 1.73 (s, *Me*$_2$Ti, 3H), 1.10−1.59 (m, CH*Me*$_2$ and C(*^{t}Bu*)CHC(*^{t}Bu*), 42H). ^{13}C NMR (25 °C, 100.6 MHz, THF-d_8): δ 173.6 (*C*(^{t}Bu)CHC(^{t}Bu)), 150.3 (C_6H_3), 147.2 (C_6H_3), 144.7 (C_6H_3), 142.3 (C_6H_3), 139.7 (C_6H_3), 136.0 (C_6H_3), 127.0 (C_6H_3), 125.2 (C_6H_3), 124.4 (C_6H_3), 121.3 (C_6H_3), 118.1 (C_6H_3), 114.9 (C_6H_3), 97.0 (C(^{t}Bu)*C*HC(^{t}Bu), J_{C-H} = 160 Hz), 82.4 (*Me*$_2$Ti), 68.6 (*Me*$_2$Ti), 43.1 (C(*C*Me$_3$)CHC(CMe$_3$)), 42.3 (C(CMe$_3$)CHC(*C*Me$_3$)), 29.6 (C(C*Me*$_3$)CHC(CMe$_3$)), 28.7 (C(CMe$_3$)CHC(C*Me*$_3$)), 27.0 (br), 26.7 (br), 25.6 (br), 24.0 (br). ^{19}F NMR (23 °C, 282.3, MHz, THF-d_8): δ −78.9 (s, O_3SCF_3). Anal. Calcd for $C_{38}H_{59}N_2TiSO_3F_3$: C, 62.62; H, 8.16; N, 3.84. Found: C, 62.62; H, 8.17; N, 3.62.

Synthesis of Complex ($^{t\mathrm{Bu}}$nacnac)Ti═P[Trip](CH$_3$) (3). In a vial was dissolved ($^{t\mathrm{Bu}}$nacnac)Ti(CH$_3$)$_2$(OTf) [500 mg, 0.69 mmol] in ether (10 mL) and the solution was cooled to −35 °C. To the cold solution was added a cold ether solution (∼10 mL) containing LiPH[Trip] [166 mg, 0.69 mmol]. After stirring for 20 min the solution was dried under reduced pressure, the brown powder was extracted with hexane and filtered, and the filtrate was concentrated under reduced pressure. The concentrated solution was then cooled to −35 °C to afford large purple crystals of ($^{t\mathrm{Bu}}$nacnac)Ti═P[Trip](CH$_3$) (**3**) in two crops [325 mg, 0.41 mmol, 59.4% yield]. ^{1}H NMR (23 °C, 399.8 MHz, C_6D_6): δ 7.08−6.83 (m, C_6H_3, C_6H_2, 8H), 5.40 (s, C(^{t}Bu)C*H*C(^{t}Bu), 1H), 4.00 (septet, C*H*Me$_2$, 2H), 3.58 (septet, C*H*Me$_2$, 4H), 2.65 (septet, C*H*Me$_2$, 1H), 1.75 (d, CH*Me*$_2$, 6H), 1.42 (d, CH*Me*$_2$, 6H), 1.36 (d, CH*Me*$_2$, 6H), 1.29 (d, CH*Me*$_2$, 6H), 1.27 (s, Ti−C*H*$_3$, 3H), 1.10 (d, CH*Me*$_2$, 18H), 1.04 (s, C(*^{t}Bu*)CHC(*^{t}Bu*), 18H). ^{13}C NMR (25 °C, 100.6 MHz, C_6D_6): δ.173.7 (*C*(^{t}Bu)CH*C*(^{t}Bu)), 155.3 (ipso-C_6H_2, J_{C-P} = 28 Hz,), 149.4 (C_6H_3), 149.1 (C_6H_3), 147.0 (C_6H_3), 142.2 (C_6H_3), 140.2 (C_6H_3), 126.5 (C_6H_3), 124.1 (C_6H_3), 124.0 (C_6H_3), 119.9 (C_6H_3), 90.0 (C(^{t}Bu)*C*HC(^{t}Bu)), 45.0 (C(*C*Me$_3$)CHC(*C*Me$_3$)), 41.4 (Ti-*C*H$_3$), 34.6 (*C*HMe$_2$), 32.5 (*C*HMe$_2$), 32.0 (C(C*Me*$_3$)CHC(C*Me*$_3$)), 29.5 (*C*HMe$_2$), 29.0 (*C*HMe$_2$), 27.6 (*Me*), 25.5 (*Me*), 24.6 (*Me*), 24.5 (two *Me* groups), 24.3 (*Me*), 24.2 (*Me*). ^{31}P NMR (25 °C, 161.9 MHz, C_6D_6): δ 231.5 (s, *P*[Trip]). Anal. Calcd for $C_{51}H_{79}N_2TiP$: C, 76.66; H, 9.97; N, 3.51. Found: C, 76.71; H, 10.20; N, 3.87. UV−vis (C_6H_6, 25 °C): 315 (ϵ = 27886 L·mol^{-1}·cm^{-1}), 368 (ϵ = 13743 L·mol^{-1}·cm^{-1}), 502 (ϵ = 2237 L·mol^{-1}·cm^{-1}) nm.

Synthesis of Complex ($^{t\mathrm{Bu}}$nacnac)Ti═P[Trip]{CH$_3$B(C$_6$F$_5$)$_3$} (5). Flurobenzene was added to the mixture of ($^{t\mathrm{Bu}}$nacnac)Ti═P[Trip](CH$_3$) [1.00 g, 1.25 mmol] and $B(C_6F_5)_3$ [640 mg, 1.25 mmol]. After allowing the reaction to proceed at room temperature for 10 min, the solution was layered with pentane and cooled to −35 °C to afford large brown crystals of ($^{t\mathrm{Bu}}$nacnac)Ti═P[Trip]{$CH_3B(C_6F_5)_3$} (**5**) in two crops [1.17 g, 0.89 mmol, 71.2% yield]. ^{1}H NMR (23 °C, 399.8 MHz, C_6D_5Br): δ 7.46−6.81 (m, C_6H_3, C_6H_2 and C(^{t}Bu)C*H*C(^{t}Bu) 9H), 3.50 (septet, C*H*Me$_2$, 2H), 3.28 (septet, C*H*Me$_2$, 2H), 3.00 (septet, C*H*Me$_2$, 2H), 2.73 (septet, C*H*Me$_2$, 1H), 1.70 (d, CH*Me*$_2$, 6H), 1.41 (d, CH*Me*$_2$,6H), 1.25−0.96 (CH*Me*$_2$, C*H*$_3$, C(*^{t}Bu*)CHC(*^{t}Bu*), 51H). ^{13}C NMR (25 °C, 100.6 MHz, C_6D_5Br): δ 175.8 (*C*(^{t}Bu)CH*C*(^{t}Bu)), 153.8 (C_6H_3), 151.7 (C_6H_3), 148.8 (br, B(*C*$_6$F$_5$)$_3$), 140.9 (C_6H_3), 138.8 (C_6H_3), 136.8 (br, B(*C*$_6$F$_5$)$_3$), 131.7 (C_6H_3), 128.4 (C_6H_3), 128.0 (C_6H_3), 124.7 (C_6H_3), 124.4 (C_6H_3), 120.3 (C_6H_3), 113.6 (C(^{t}Bu)CHC(^{t}Bu)), 44.6 (C(*C*Me$_3$)-CHC(*C*Me$_3$)), 34.3 (*C*HMe$_2$), 31.8 (*C*HMe$_2$), 31.0 (*C*HMe$_2$), 30.8 (C(C*Me*$_3$)CHC(C*Me*$_3$)), 28.9 (*C*HMe$_2$), 25.3 (*Me*), 24.5 (two *Me* groups), 24.4 (*Me*), 23.7 (*Me*), 23.5 (*Me*), 23.3 (*Me*). ^{31}P NMR (25 °C, 161.9 MHz, C_6D_5F): δ 206.8 (s, *P*[Trip]). ^{19}F NMR (23 °C, 282.3 MHz, C_6D_5Br): δ −131.8 (B(*C*$_6$F$_5$)$_3$), −164.9 (B(*C*$_6$F$_5$)$_3$), −166.6 (B(*C*$_6$F$_5$)$_3$). ^{11}B NMR (23 °C, 128.4 Hz, C_6D_5Br): δ −14.2 (*B*(*C*$_6$F$_5$)$_3$). UV−vis (C_6H_6, 25 °C): 315 (ϵ = 3718 L·mol^{-1}·cm^{-1}), 365 (ϵ = 3974 L·mol^{-1}·cm^{-1}), 500 (broad shoulder) nm. Multiple attempts to obtain satisfactorily elemental analysis have failed presumably because of the thermal sensitivity of **4**.

Synthesis of Complex [($^{t\mathrm{Bu}}$nacnac)Ti(P[Trip]PhCCPh)][CH$_3$B-(C$_6$F$_5$)$_3$] (6). C_6D_5Br was added to the mixture of **4** [75.7 mg, 0.06 mmol] and PhCCPh [10.8 mg, 0.06 mmol] in a J. Yong NMR tube. After allowing the reaction to proceed at room temperature for 10 min, the crude NMR spectrum revealed quantitative formation of [($^{t\mathrm{Bu}}$nacnac)-Ti(P[Trip]PhCCPh)][$CH_3B(C_6F_5)_3$] (**5**). ^{1}H NMR (23 °C, 399.8 MHz, C_6D_5Br): δ 7.30−6.38 (m, aryl, 18H), 6.04 (C(^{t}Bu)C*H*C(^{t}Bu),1H), 2.82 (septet, C*H*Me$_2$, 2H), 2.41(mixture of septets, C*H*Me$_2$, 3H), 1.88 (septet, C*H*Me$_2$, 2H), 0.96 (d, CH*Me*$_2$, 12H), 0.93 (s, C*H*$_3$, 3H), 0.85 (d, CH*Me*$_2$, 12H), 0.78 (s, C(*^{t}Bu*)CHC(*^{t}Bu*), 18H), 0.71 (d, CH*Me*$_2$, 6H), 0.41 (d, CH*Me*$_2$, 6H), 0.22 (d, CH*Me*$_2$, 6H), ^{13}C NMR (25 °C, 100.6 MHz, C_6D_5Br): δ 253.5 (Ti-*C*PhCPh), 175.3 (*C*(^{t}Bu)CH*C*(^{t}Bu), 156.9, 156.4, 148.8 ($CH_3B(C_6F_5)_3$), 142.3, 140.6, 140.5, 140.0, 137.7 ($CH_3B(C_6F_5)_3$), 136.6 ($CH_3B(C_6F_5)_3$), 133.4, 131.7, 130.1, 129.1, 128.9, 128.7, 128.4, 128.3, 126.1, 124.7, 124.5, 122.8, 115.2, 88.6 (C(^{t}Bu)*C*HC(^{t}Bu)), 45.1 (C(*C*Me$_3$)CHC(*C*Me$_3$)), 34.6 (*C*HMe$_2$), 34.3 (*C*HMe$_2$), 31.0 (C(C*Me*$_3$)-CHC(C*Me*$_3$)), 29.3 (*C*HMe$_2$), 28.2 (*C*HMe$_2$), 26.0 (*Me*), 25.8 (*Me*), 25.0 (*Me*), 24.1 (*Me*), 24.0 (*Me*), 23.4 (*Me*), 21.6 (*Me*). ^{31}P NMR (25 °C,

161.9 MHz, C_6D_5Br): δ 160.7 (s, *P*[Trip]). ^{19}F NMR (23 °C, 282.3 Hz, C_6D_5Br): δ −132.7 ($CH_3B(C_6F_5)_3$), −165.3 ($CH_3B(C_6F_5)_3$), -167.7 ($CH_3B(C_6F_5)_3$). ^{11}B NMR (23 °C,128.4 MHz, C_6D_5Br): δ −14.9 ($CH_3B(C_6F_5)_3$). Anal. Calcd for $C_{83}H_{89}N_2TiPBF_{15}$: C, 66.94; H, 6.02; N, 1.88. Found: C, 66.44; H, 6.07; N, 1.94.

Treatment of 6 with H_2NPh to form HP[Trip]PhC═CHPh. To a stirring solution of **6** in fluorobenzene was added 1.2 equiv of aniline. The solution was allowed to stir for 4 h after which, the solvent was removed under vacuo. The organic product was extracted from the remaining brown residue with hexane. The hexane solution was filtered and dried under reduced pressure resulting in a yellow oil. ^1H NMR (25 °C, 499.8 MHz, C_6D_{12}): δ 7.40 (m, aryl, 1), 7.15 (m, aryl, 5), 7.07 (s, aryl, 2), 6.86 (m, aryl, 3), 6.73 (m, aryl, 2), 6.19 (d, J_{P-H} = 6 Hz, *H*C═C, 1), 4.80 (d, J_{P-H} = 221 Hz, P*H*, 1), 3.77 (septet, C*H*Me_2, 2H), 2.86 (septet, C*H*Me_2, 1H), 1.26 (d, CH_3, 12H), 1.18 (d, CH_3, 6H). ^{13}C NMR (25 °C, 125.69 MHz, C_6D_{12}): δ 155.01 (J_{P-C} = 14 Hz), 151.23, 142.14 (J_{P-C} = 15 Hz) 141.77 (J_{P-C} = 21 Hz), 137.88, 133.68 (J_{P-C} = 17 Hz), 132.16, 129.52, 129.03, 128.68 (J_{P-C} = 4 Hz), 128.49, 128.14, 127.33, 122.03, 35.40 (*C*HMe_2), 35.67 (d, *C*HMe_2, J_{P-C} = 14 Hz,), 25.28 (CH*Me*$_2$), 24.70 (CH*Me*$_2$), 24.29 (CH*Me*$_2$). ^{31}P NMR (25 °C, 161.9 MHz, C_6D_6): δ −62.72 (s, *P*[Trip]). MS-EI: M^+ = 414.25.

Crystallographic Details. Inert atmosphere techniques were used to place the crystal onto the tip of a diameter glass capillary (0.03−0.20 mm) and mounted on a SMART6000 (Bruker) at 113−140 K. A preliminary set of cell constants was calculated from reflections obtained from three nearly orthogonal sets of 20−30 frames. Data collections were carried out using graphite monochromated Mo Kα radiation with a frame time of 3 s with a detector distance of 5.0 cm. A randomly oriented region of a sphere in reciprocal space was surveyed. Three sections of 606 frames were collected with 0.30° steps in ω at different ϕ settings with the detector set at −43° in 2θ. Final cell constants were calculated from the *xyz* centroids of strong reflections from the actual data collection after integration (SAINT).[59] The structure was solved using SHELXS-97 and refined with SHELXL-97.[60] A direct-methods solution was calculated which provided most non-hydrogen atoms from the E-map. Full-matrix least squares/difference Fourier cycles were performed which located the remaining non-hydrogen atoms. All non-hydrogen atoms were refined with anisotropic displacement parameters, and all hydrogen atoms were refined with isotropic displacement parameters (unless otherwise specified, vide infra). A summary of crystal data and refinement details for all structures are given in Table 5.

(1)·C_6H_{14}. A dark crystal of approximate dimensions 0.30 × 0.25 × 0.25 mm^3 was selected and mounted on a glass fiber. A total of 11975 reflections (−13 ≤ *h* ≤ 17, −27 ≤ *k* ≤ 8, −22 ≤ *l* ≤ 24) were collected at *T* = 125(2) K in the range of 2.03−27.52° of which 7099 were unique (R_{int} = 0.0472); Mo Kα radiation (λ = 0.71073 Å). A direct-methods solution was calculated which provided most non-hydrogen atoms from the E-map. All non-hydrogen atoms were refined with anisotropic displacement parameters. A disordered hexane solvent is located in the unit cell. The residual peak and hole electron densities were 0.317 and −0.341 eÅ^{-3}. The absorption coefficient was 0.223 mm^{-1}. The least squares refinement converged normally with residuals of R(*F*) = 0.0426, wR(F^2) = 0.0658, and a GOF = 0.797 ($I > 2\sigma(I)$); $C_{58}H_{94}N_2PTi$; space group *P*2(1)/*n*; monoclinic; *a* = 13.85(8), *b* = 21.04(2), *c* = 18.74(3), β = 93.21(8)°; *V* = 5453(12) A^3; *Z* = 4; D_{calcd} = 1.094 mg/m^3; *F*(000) = 1972.

(3). A dark brown crystal of approximate dimensions 0.30 × 0.25 × 0.25 mm^3 was selected and mounted on a glass fiber. A total of 11176 reflections (−13 ≤ *h* ≤ 14, −27 ≤ *k* ≤ 27, −25 ≤ *l* ≤ 27) were collected at *T* = 120(2) K in the range of 2.11 to 27.55° of which 7118 were unique (R_{int} = 0.0868); Mo Kα radiation (λ = 0.71073 Å). A direct-methods solution was calculated which provided most non-hydrogen atoms from the E-map. All non-hydrogen atoms were refined with anisotropic displacement parameters. The residual peak and hole electron densities were 0.345 and −0.257 eA^{-3}. The absorption coefficient was 0.242 mm^{-1}. The least squares refinement converged normally with residuals of R(*F*) = 0.0442, wR(F^2) = 0.0977, and a GOF = 0.911 ($I > 2\sigma(I)$); $C_{51}H_{79}N_2PTi$; space group *P*2(1)/*n*; monoclinic; *a* = 11.104(2), *b* = 21.191(4), *c* = 21.135(4), β = 102.302-(5)°; *V* = 4859.2(16) Å^3; *Z* = 4; D_{calcd} = 1.092 mg/m^3; *F*(000) = 1744.

Table 5. Summary of Crystallographic Data and Structure Refinement for Complexes **1**·C_6H_{14}, **3**, and **4**·1.5FC_6H_5

	1·C_6H_{14}	**3**	**4**·1.5FC_6H_5
formula	$C_{58}H_{94}N_2PTi$	$C_{51}H_{79}N_2PTi$	$C_{78}H_{85}BF_{16.57}N_2PTi$
FW	898.22	799.03	1455.04
space group	*P*2(1)/*n*	*P*2(1)/*n*	*P*2(1)/*c*
a (Å)	13.854(18)	11.104(2)	14.5495(10)
b (Å)	21.04(2)	21.191(4)	20.0614(14)
c (Å)	18.74(3)	21.135(4)	24.8462(17)
α (deg)	90.00	90.00	90.00
β (deg)	93.21(8)	102.302(5)	90.677(2)
γ (deg)	90.00	90.00	90.00
V (Å^3)	5453(12)	4859.2(16)	7251.7(9)
Z	4	4	4
D_{calcd}	1.094	1.092	1.333
linear abs coeff	0.223	0.242	0.227
F(000)	1972	1744	3033
cryst color/solvent	deep red hexane	dark brown hexane	deep red FC_6H_5/ hexane
cryst form	irregular	multifaceted	irregular fragment
cryst size (mm)	0.30 × 0.25 × 0.25	0.30 × 0.30 × 0.25	0.30 × 0.30 × 0.25
Θ range (lattice, deg)	2.03−27.52	2.11−27.55	2.14−30.03
index range	−13 ≤ *h* ≤ 17 −27 ≤ *k* ≤ 8 −22 ≤ *l* ≤ 24	−13 ≤ *h* ≤ 14 −27 ≤ *k* ≤ 27 −25 ≤ *l* ≤ 27	−20 ≤ *h* ≤ 20 −28 ≤ *k* ≤ 28 −34 ≤ *l* ≤ 34
reflns collected	18817	34306	164162
unique reflns $F > 4\sigma(F)$	11975	11176	21184
obsd reflns	7099	7118	14120
R_{int}	0.0472	0.0868	0.0767
Final R indices [$I > 2\sigma(I)$]	R1 = 0.0426 wR2 = 0.0658	R1 = 0.0442 wR2 = 0.0977	R1 = 0.0367 wR2 = 0.0846
R indices (F^2, all data)	R1 = 0.0815 wR2 = 0.0735	R1 = 0.0815 wR2 = 0.1097	R1 = 0.0666 wR2 = 0.0942
GOF on F^2	0.797	0.911	0.935

(4)·1.5FC_6H_5. A deep red crystal of approximate dimensions 0.30 × 0.30 × 0.25 mm^3 was selected and mounted on a glass fiber. A total of 21184 reflections (−20 ≤ *h* ≤ 20, −28 ≤ *k* ≤ 28, −34 ≤ *l* ≤ 34) were collected at *T* = 119(2) K in the range of 2.14 to 30.03° of which 14120 were unique (R_{int} = 0.0767); Mo Kα radiation (λ = 0.71073 Å). A direct-methods solution was calculated which provided most non-hydrogen atoms from the E-map. All non-hydrogen atoms were refined with anisotropic displacement parameters. Two FC_6H_5 solvent molecules are present, both slightly disordered and one lying at a symmetry site. The residual peak and hole electron densities were 0.499 and −0.297 eÅ^{-3}. The absorption coefficient was 0.227 mm^{-1}. The least squares refinement converged normally with residuals of R(*F*) = 0.0367, wR(F^2) = 0.0846, and a GOF = 0.935 ($I > 2\sigma(I)$); $C_{78}H_{85}BF_{16.57}N_2PTi$; space group *P*2(1)/*c*; monoclinic; *a* = 14.550(1), *b* = 20.061(4), *c* = 24.846(7), β = 90.677(2)°; *V* = 7251.7(9) Å^3; *Z* = 4, D_{calcd} = 1.333 mg/m^3, *F*(000) = 3033.

Computational Details. All calculations were carried out using density functional theory as implemented in the Jaguar 5.5 suite[25] of ab initio quantum chemistry programs. Geometry optimizations were performed with the B3LYP[26] functional and the 6-31G** basis set. Titanium was represented using the Los Alamos LACVP basis.[27] The bond order is calculated using the definition of Mayer.[28] Geometry optimizations have been carried out beginning with the crystal structures for complexes **1**, **3**, and **4**, and without symmetry restrictions, and optimized geometries are in good agreement with the X-ray structures. The full models consist of 134−168 atoms which represent the nonsimplified ligands that were also used in the experimental portion of this work. These calculations challenge the current state of

(59) *SAINT 6.1*; Bruker Analytical X-ray Systems: Madison, WI.
(60) *SHELXTL-Plus*, version 5.10; Bruker Analytical X-ray Systems: Madison, WI.

computational capabilities, whereas the numerical efficiency of the Jaguar program allows us to accomplish this task in a bearable time frame.

Catalytic Reactions Hydrophosphination and Carboamination of PhCCPh. Hydrophosphination. In a typical experiment, **4** [0.025 mmol, 10 mol %], alkyne [0.275 mmol], and H_2PPh [0.25 mmol] were mixed in a J. Young NMR tube in C_6D_6 (0.8 mL) inside the glovebox. The NMR tube was removed from the glovebox and was heated to ~80 °C for approximately 14−16 h. The reaction progress was monitored by ^1H and ^{31}P NMR spectroscopy. After the reaction was completed, the NMR tube was cooled to room temperature, the product purified by silica gel column chromatography (under an inert atmosphere) to afford the secondary vinylphosphine HP[Phenyl]PhC═CHPh as a mixture of *E* and *Z* isomers [58 mg, 73% yield].

Major Isomer. ^1H NMR (25 °C, 300.059 MHz, C_6D_6): 7.5−6.8 (m, aryl-*H*), 7.06 (d, J_{P-H} = 13.5 Hz vinyl-*H*, 1H), 5.07 (d, J_{P-H} = 218 Hz, P-*H*, 1H). $^{31}P[^1H]$ NMR (25 °C, 161.9 MHz, C_6D_6): δ −16.40 (s, Ar-*P*). MS-CI: MH^+ = 289.11, and GC−MS M^+ = 288.

Minor Isomer. ^1H NMR (25 °C, 300.059 MHz, C_6D_6): 7.5−6.8 (m, aryl-*H*), 7.25 (d, J_{P-H} = 16.6 Hz, vinyl-*H*, 1H), 5.38 (d, J_{P-H} = 224 Hz, P-*H*, 1H). $^{31}P[^1H]$ NMR (25 °C, 161.9 MHz, C_6D_6): δ −52.78 (s, Ar-*P*). MS-CI: MH^+ = 289.11, and GC−MS M^+ = 288.

Mixture of *E* + *Z* Isomers. ^{13}C NMR (25 °C, 100.6 MHz, C_6D_{12}): δ 145.5, 141.7, 141.0, 140.2, 139.0, 138.4, 138.3, 137.7, 137.6, 137.1, 134.6, 134.2, 133.4, 131.9, 130.6, 129.7, 129.6, 129.2, 129.1, 128.9, 128.7, 128.6, 128.5, 128.4, 128.3, 127.9, 127.3, 126.9.

Carboamination. In a typical experiment, **4** [0.025 mmol, 10%], alkyne [0.275 mmol], and aldimine [**6a**−**c**, 0.25 mmol] were mixed in a J. Young NMR tube in C_6D_6 (0.8 mL) inside the glovebox. The NMR tube was removed from the glovebox and was heated at 125 °C. The reaction progress was monitored by ^1H NMR spectroscopy. After the reaction was completed, the NMR tube was cooled to room temperature, and the product purified by silica gel column chromatography (5% ether/hexanes) to afford yellow α,β-unsaturated imine product (**7a**−**c**, 68−70% yield). ^1H and ^{13}C NMR spectra of α,β-unsaturated imine product were compared to samples prepared independently.[49] NOTE: It is imperative that both substrates and inert atmospheres be free of moisture, oxygen, coordinating solvents (Et_2O, THF, pyridine, etc), and Cl sources (CH_2Cl_2, $CHCl_3$, CCl_4, etc). Traces of these elements will reduce the catalytic activity. It is highly recommended that substrates, solvents, and titanium precursors be freed of coordinating solvents prior to usage in catalytic reactions.

Acknowledgment. This work was supported by Indiana University, the Camille and Henry Dreyfus Foundation (Teacher-Scholar Award to D.J.M.), the Alfred P. Sloan Foundation (Fellowship to D.J.M.), and the National Science Foundation (Grant CHE-0348941 and PECASE award to D.J.M.). G.W. thanks the Natural Sciences and Engineering Research Council (NSERC) of Canada for research and equipment grants. The authors would like to thank the referees for helpful suggestions.

Supporting Information Available: Complete crystallographic data for compounds **1**, **3**, and **4** (CIF files) and complete geometrical parameters for their optimized geometries. This material is available free of charge via the Internet at http://pubs.acs.org.

JA064853O